

A stabilization method of F-barES-FEM-T4 for dynamic explicit analysis of nearly incompressible solids

Ryoya Iida^{1,a)}, Yuki Onishi¹ and Kenji Amaya¹

¹ Department of Systems and Control Engineering, Tokyo Institute of Technology, Japan

^{a)}Corresponding and Presenting author: riida@a.sc.e.titech.ac.jp

Abstract

SymF-barES-FEM-T4 is proposed in order to ensure the stability of F-barES-FEM-T4 in dynamic analysis. This formulation aims to symmetrize stiffness matrix of F-barES-FEM-T4 so as to remove unstable deformation modes. The modification for stabilization is restricted to the internal force vector and does not cause increase of degrees of freedom (DOF). An example of analysis reveals that SymF-barES-FEM-T4 can show the comparable deformed shapes and acceptable pressure distributions without energy divergence, which cannot be realized by F-barES-FEM-T4. It also reveals that increase of the number of cyclic smoothings for SymF-barES-FEM-T4 does not always improve the pressure distributions no longer unlike F-barES-FEM-T4.

Introduction

The tetrahedral elements are the current only choice in finite element (FE) analysis for complex structures due to their ease of mesh generation. However, conventional tetrahedral FE formulations easily cause locking and pressure oscillation in nearly incompressible cases. The high-order formulations can resolve only shear locking but still suffer from volumetric locking and pressure oscillation. The u/p hybrid formulations[1], which is widely used to overcome incompressibility, are applicable only in implicit cases but inapplicable in explicit dynamics. Thus, FE formulations for dynamic explicit analysis of nearly incompressible materials with 4-node tetrahedral (T4) elements are still in research stage.

Recently, some T4 elements featured with the idea of smoothed finite element methods (S-FEMs)[2] have been proposed in order to realize explicit dynamics of nearly incompressible materials. Selective ES/NS-FEM-T4[3, 4, 5, 6, 7] decomposes Cauchy stress tensor into hydrostatic part and deviatoric part, which are derived from NS-FEM-T4 and ES-FEM-T4 respectively. Although it can analyze deformation without locking, it cannot completely overcome pressure oscillation. F-barES-FEM-T4[8, 9] decomposes deformation gradient into isovolumetric part and volumetric part in the same manner as F-bar method[10]. Isovolumetric part is derived in the same as ES-FEM-T4 and volumetric part is derived by smoothing between nodes and elements in a few times. This formulation can completely overcome locking and pressure oscillation in static analysis and be expected to show the same ability in explicit dynamics.

Our group extended F-barES-FEM-T4 to explicit dynamics in previous work[11]. The results can show comparable pressure distribution and deformed shapes without locking. However, they also revealed instability of F-barES-FEM-T4 in dynamic problems due to their imaginary parts of eigenfrequencies raised by the asymmetric stiffness matrix; therefore, high-accurate results are restricted to short-term analysis.

This paper proposes a stabilized F-barES-FEM-T4, named SymF-barES-FEM-T4. The idea for stabilization is to symmetrize stiffness matrix of F-barES-FEM-T4 by replacing the formula to derive the internal force. In the following sections, the outline and an example of analysis for SymF-barES-FEM-T4 are explained. An example for explicit dynamics of nearly incompressible materials illustrates the stability and accuracy of SymF-barES-FEM-T4.

Methods

This section explains the outline of F-barES-FEM-T4 and that of proposed method named SymF-barES-FEM-T4.

Outline of F-barES-FEM-T4

F-barES-FEM-T4 is designed in order to realize highly accurate analysis for nearly incompressible materials. This formulation uses the ideas of F-bar method[10] and S-FEMs[2]. At first, deformation gradients at h -th edge ${}^{\text{Edge}}_h\bar{\mathbf{F}}$ are decomposed into isovolumetric part ${}^{\text{Edge}}_h\bar{\mathbf{F}}^{\text{iso}}$ and volumetric part ${}^{\text{Edge}}_h\bar{\mathbf{F}}^{\text{vol}}$ in the same manner as F-bar method:

$${}^{\text{Edge}}_h\bar{\mathbf{F}} = {}^{\text{Edge}}_h\bar{\mathbf{F}}^{\text{iso}} \cdot {}^{\text{Edge}}_h\bar{\mathbf{F}}^{\text{vol}}. \quad (1)$$

${}^{\text{Edge}}_h\bar{\mathbf{F}}^{\text{iso}}$ is calculated in the same manner as ES-FEM-T4, namely,

$${}^{\text{Edge}}_h\bar{\mathbf{F}}^{\text{iso}} = {}^{\text{Edge}}_h\bar{\mathbf{F}}^{\text{iso}} = \frac{1}{{}^{\text{Edge}}_h\bar{\mathbf{J}}^{1/3}} {}^{\text{Edge}}_h\bar{\mathbf{F}}, \quad (2)$$

where $\bar{\square}$ denotes the smoothed value at an edge and ${}^{\text{Edge}}_h\bar{\mathbf{J}}$ is relative volume change at h -th edge calculated as $\det({}^{\text{Edge}}_h\bar{\mathbf{F}})$. Meanwhile, volumetric part ${}^{\text{Edge}}_h\bar{\mathbf{F}}^{\text{vol}}$ is derived from the weighted mean of neighboring elements' relative volume change ${}^{\text{Elem}}J$. Weight values are defined by cyclic smoothing among nodes and elements. More concrete procedure is described in [8, 9, 11]. The smoothed Cauchy stress tensor at h -th edge ${}^{\text{Edge}}_h\bar{\mathbf{T}}$ is derived from ${}^{\text{Edge}}_h\bar{\mathbf{F}}$ and material constitutive model. The nodal force vector at h -th edge ${}^{\text{Edge}}_h\bar{\mathbf{f}}^{\text{int}}$ is calculated as following:

$${}^{\text{Edge}}_h\bar{\mathbf{f}}^{\text{int}}_{P:p} = \frac{\partial {}^{\text{Edge}}_h\bar{\mathbf{D}}_{ij}}{\partial u_{P:p}} {}^{\text{Edge}}_h\bar{\mathbf{T}}_{ij} {}^{\text{Edge}}_h\bar{V}, \quad (3)$$

where $\square_{P:p}$ indicates p -th direction of P -th nodal value, u is nodal displacement, $\dot{\square}$ indicates time derivative value, ${}^{\text{Edge}}_h\bar{\mathbf{D}}$ is stretching tensor derived from ${}^{\text{Edge}}_h\bar{\mathbf{F}}$ and ${}^{\text{Edge}}_h\bar{V}$ is assigned volume to h -th edge.

Outline of SymF-barES-FEM-T4

According to [11], F-barES-FEM-T4 holds instability in dynamic analysis due to the imaginary parts of eigenfrequencies. Such imaginary parts are caused by asymmetry of the stiffness matrix in small deformation analysis. To ensure the stability in dynamic analysis, we modify ${}^{\text{Edge}}_h\bar{\mathbf{f}}^{\text{int}}$ in the following manner[12]:

$${}^{\text{Edge}}_h\bar{\mathbf{f}}^{\text{int}}_{P:p} = \frac{\partial {}^{\text{Edge}}_h\bar{\mathbf{D}}_{ij}}{\partial u_{P:p}} {}^{\text{Edge}}_h\bar{\mathbf{T}}_{ij} {}^{\text{Edge}}_h\bar{V}, \quad (4)$$

where stretching tensor ${}^{\text{Edge}}_h\bar{\mathbf{D}}$, derived from ${}^{\text{Edge}}_h\bar{\mathbf{F}}$, is used instead of ${}^{\text{Edge}}_h\bar{\mathbf{D}}$. This formulation, named SymF-barES-FEM-T4, ensures the symmetry of stiffness matrix in small deformation case; therefore, it can be expected that unstable deformation modes of F-barES-FEM-T4 are removed. Details of derivation for each term are summarized in [9].

Since this modification is restricted to the stretching tensor, SymF-barES-FEM-T4 can be formulated without increasing DOF and restrictions on material constitutive models as well as F-barES-FEM-T4. However, the calculation cost for internal force vector is more expensive than F-barES-FEM-T4.

Results

Figure 1 illustrates the outline of dynamic bending analysis for cantilever. The shape of cantilever is defined as $10 \times 1 \times 1$ m cuboid; its left side is perfectly constrained; a uniform initial velocity of 2.0 m/s in $-z$ direction is applied. The material constitutive model is Neo-Hookean hyperelastic model. The density, initial Young's modulus and initial Poisson's ratio are 920 kg/m^3 , 6.0 MPa and 0.49, respectively. The analyses with ABAQUS/Explicit C3D4, Selective ES/NS-FEM-T4, SymF-barES-FEM-T4 and F-barES-FEM-T4 are performed with unstructured tetrahedral elements of 0.2 m global mesh seed size. The analysis with ABAQUS/Explicit C3D8 of 0.2 m global mesh seed size is also performed to obtain a reference solution. The number of cyclic smoothings c is 1 to 3, in the analyses with SymF-barES-FEM-T4 and F-barES-FEM-T4. All results of SymF-barES-FEM-T4 and F-barES-FEM-T4 are labeled with (c) such as "F-barES-FEM-T4(c)". In these analyses, the time integration scheme is Velocity Verlet, and the time increment is 1.0×10^{-4} s.

The comparison of the vertical displacements (u_z) at one of the corner node (\bigcirc in Figure 1) is shown in Figure 2. Time histories of SymF-barES-FEM-T4s and F-barES-FEM-T4s agree with the reference in almost the same level; therefore, it

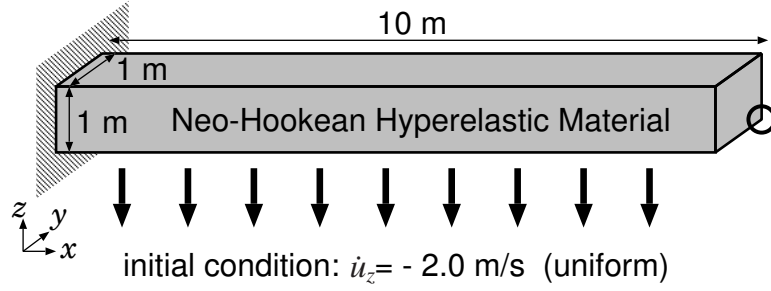


Figure 1. Outline of the dynamic bending analysis of a cantilever. The initial uniform velocity is -2.0 m/s in z direction.

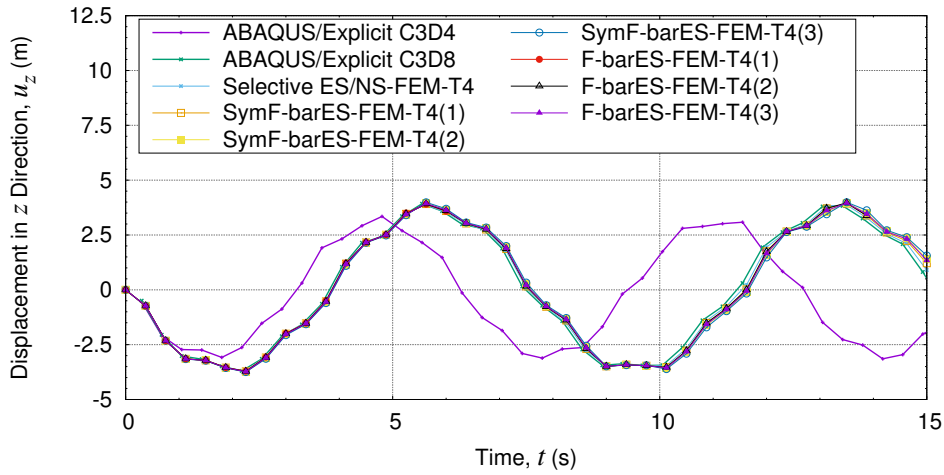


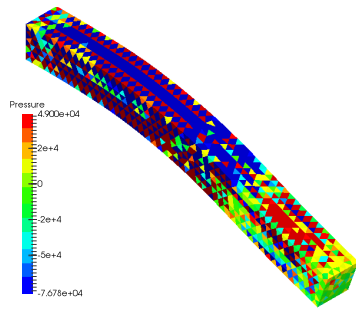
Figure 2. Comparison of the vertical displacement at the corner vs. time in the cantilever bending analysis.

can be concluded that symmetrization of SymF-barES-FEM-T4 doesn't spoil the locking-free property of F-barES-FEM-T4. Meanwhile, the result of ABAQUS/Explicit C3D4 shows far different time history due to the locking.

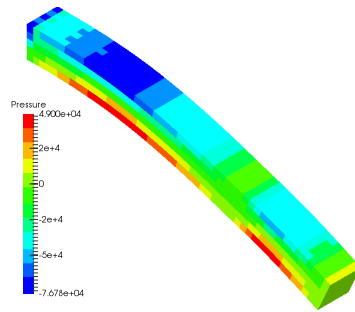
Figure 3 and 4 show the pressure distributions at 0.75 s and 4.50 s respectively. In these figures, the value above the range is colored in dark red, the one below the range is colored in dark blue and the contour ranges are [49.0, -76.8] (kPa) for 0.75 s and [0.10, -0.10] (MPa) for 4.50 s. The results of F-barES-FEM-T4 show comparable pressure distributions to the one of ABAQUS/Explicit C3D8 and increase of c improve the pressure oscillation. However, in Figure 4, F-barES-FEM-T4(1) shows the worst pressure distribution due to the energy divergence. F-barES-FEM-T4 cannot be applied to long-term analyses since they causes energy divergence in relative earlier stage than other formulation in this way.

SymF-barES-FEM-T4 can suppress pressure oscillation in the same level as not F-barES-FEM-T4 but slightly better than Selective ES/NS-FEM-T4 and increase of c does not improve pressure distribution no longer unlike F-barES-FEM-T4. Meanwhile, their accuracies are not spoiled even in Figure 4 since SymF-barES-FEM-T4 does not cause energy divergence.

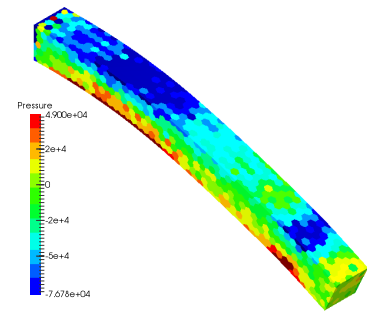
Figure 5 illustrates the time histories of total energies for each formulation. SymF-barES-FEM-T4 does not cause energy divergence although F-barES-FEM-T4(1) and (2) cause energy divergence within this analysis time. This fact indicates symmetrization can suppress unstable deformation modes of F-barES-FEM-T4.



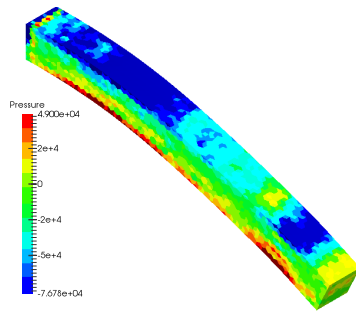
ABAQUS/Explicit C3D4



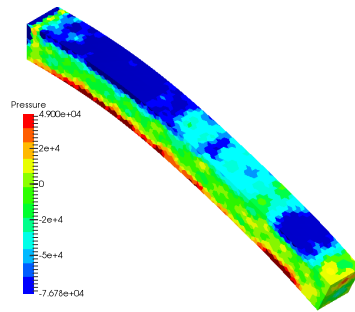
ABAQUS/Explicit C3D8



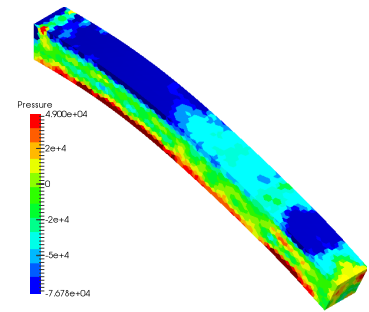
Selective ES/NS-FEM-T4



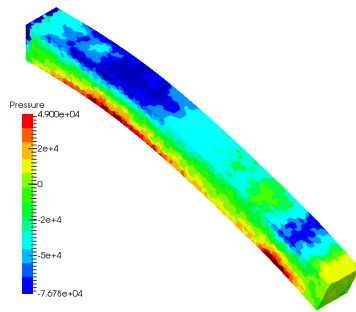
SymF-barES-FEM-T4(1)



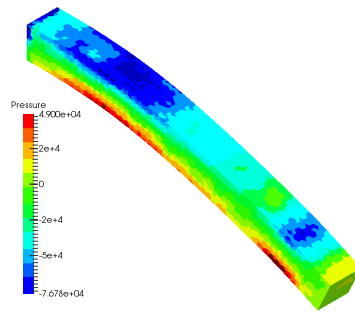
SymF-barES-FEM-T4(2)



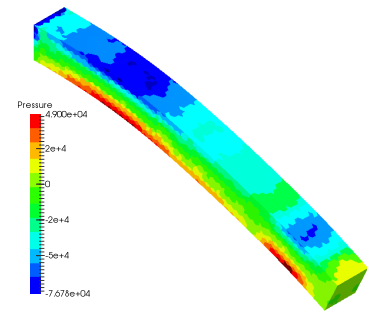
SymF-barES-FEM-T4(3)



F-barES-FEM-T4(1)

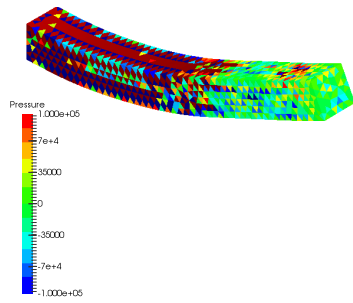


F-barES-FEM-T4(2)

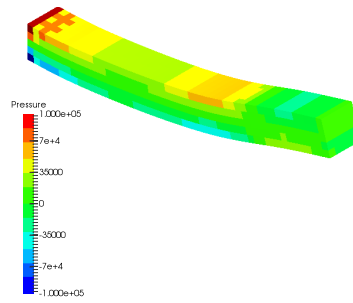


F-barES-FEM-T4(3)

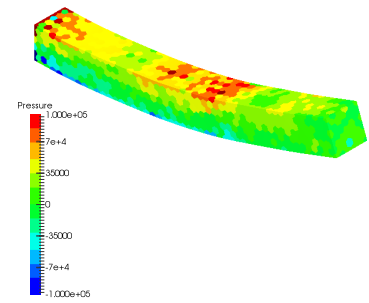
Figure 3. Deformed shapes and pressure distributions of the dynamic cantilever bending analysis at 0.75 s.



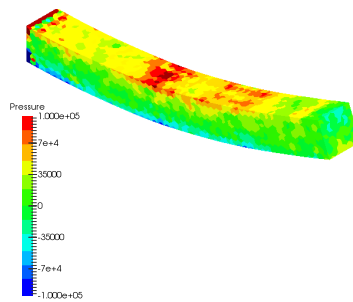
ABAQUS/Explicit C3D4



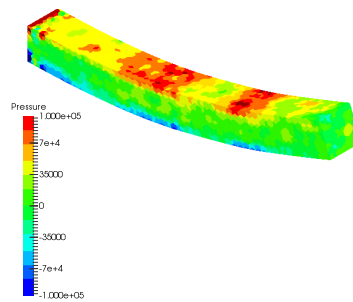
ABAQUS/Explicit C3D8



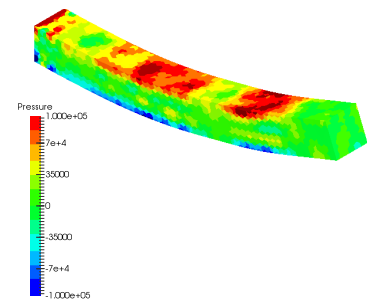
Selective ES/NS-FEM-T4



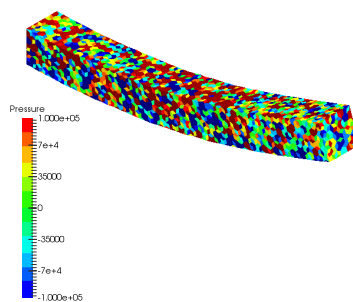
SymF-barES-FEM-T4(1)



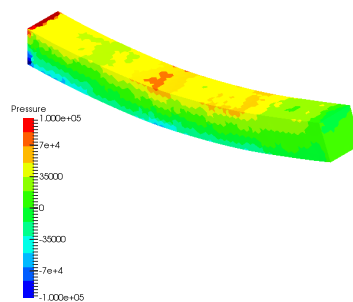
SymF-barES-FEM-T4(2)



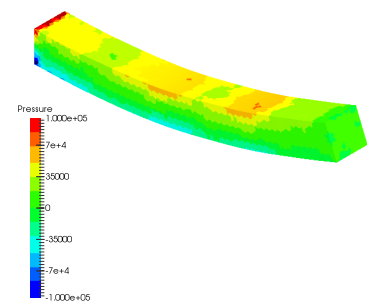
SymF-barES-FEM-T4(3)



F-barES-FEM-T4(1)



F-barES-FEM-T4(2)



F-barES-FEM-T4(3)

Figure 4. Deformed shapes and pressure distributions of the dynamic cantilever bending analysis at 4.50 s.

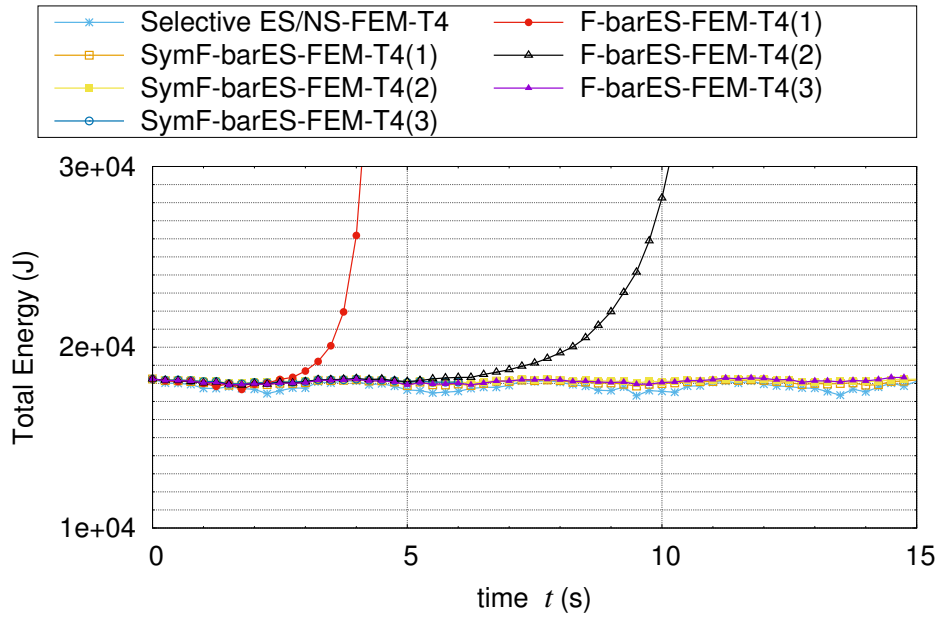


Figure 5. Time histories of the total energies for each formulation.

Conclusion

We propose stabilized F-barES-FEM-T4, named SymF-barES-FEM-T4, to realize long-term analysis for nearly incompressible materials. The advantages of SymF-barES-FEM-T4 are summarized in the followings:

- ✓ This formulation has following advantages which F-barES-FEM-T4 also has:
 - ✓ no increasing of DOF
 - ✓ no restrictions for material constitutive model
- ✓ Applicable for long-term analysis, which cannot be realized by F-barES-FEM-T4

The disadvantages of SymF-barES-FEM-T4 are summarized in the followings:

- ✗ Increasing of the number of cyclic smoothings does not improve pressure distributions unlike F-barES-FEM-T4
- ✗ suppression for pressure oscillation is worse than F-barES-FEM-T4

References

- [1] Dassault Systèmes Simulia Corp. *ABAQUS 6.13 Theory Guide*. Dassault Systèmes Simulia Corp., Providence, RI, USA, 2013.
- [2] G R Liu and T Nguyen-Thoi. *Smoothed Finite Element Methods*. CRC Press, Boca Raton, FL, USA, 2010.
- [3] Eric Li, Zhongpu Zhang, C.C. Chang, G.R. Liu, and Q. Li. Numerical homogenization for incompressible materials using selective smoothed finite element method. *Composite Structures*, 123:216 – 232, 2015.
- [4] Nguyen-Xuan Hung, Stéphane Pierre Alain Bordas, and Nguyen-Dang Hung. Addressing volumetric locking and instabilities by selective integration in smoothed finite elements. *Communications in Numerical Methods in Engineering*, 25(1):19–34, 2009.
- [5] Chen Jiang, Zhi-Qian Zhang, Xu Han, and Gui-Rong Liu. Selective smoothed finite element methods for extremely large deformation of anisotropic incompressible bio-tissues. *International Journal for Numerical Methods in Engineering*, 99(8):587–610, 2014.
- [6] Y. Onishi and K. Amaya. A locking-free selective smoothed finite element method using tetrahedral and triangular elements with adaptive mesh rezoning for large deformation problems. *International Journal for Numerical Methods in Engineering*, 99(5):354–371, 2014.
- [7] Yuki Onishi and Kenji Amaya. Performance evaluation of the selective smoothed finite element methods using tetrahedral elements with deviatoric/hydrostatic split in large deformation analysis. *Theoretical and Applied Mechanics Japan*, 63:55–65, 2015.

- [8] Y. Onishi and K. Amaya. F-bar aided edge-based smoothed finite element method with tetrahedral elements for large deformation analysis of nearly incompressible materials. *The 6th International Conference on Computational Methods*, 2015.
- [9] Y. Onishi, R. Iida, and K. Amaya. F-bar aided edge-based smoothed finite element method using tetrahedral elements for finite deformation analysis of nearly incompressible solids. *Int. J. Numer. Meth. Engng.*, 2016.
- [10] E.A. de Souza Neto, D. Peric, M. Dutko, and D.R.J. Owen. Design of simple low order finite elements for large strain analysis of nearly incompressible solids. *International Journal of Solids and Structures*, 33(20-22):3277–3296, 1996.
- [11] R Iida and Y. Onishi K. Amaya. Performance evaluation of various smoothed finite element methods with tetrahedral elements in large deformation dynamic analysis. *The 7th International Conference on Computational Methods*, 2016.
- [12] Thomas Elguedj, Yuri Bazilevs, Victor M Calo, and Thomas JR Hughes. B-bar and f-bar projection methods for nearly incompressible linear and non-linear elasticity and plasticity using higher-order nurbs elements. *Computer methods in applied mechanics and engineering*, 197(33):2732–2762, 2008.